ACS APPLIED MATERIALS & INTERFACES

Research Article

www.acsami.org

# Facile Preparation of One-Dimensional Wrapping Structure: Graphene Nanoscroll-Wrapped of $Fe_3O_4$ Nanoparticles and Its Application for Lithium-Ion Battery

Jinping Zhao,[†] Bingjun Yang,[†] Zongmin Zheng,[†] Juan Yang,[†] Zhi Yang,[†] Peng Zhang,[†] Wencai Ren,[‡] and Xingbin Yan*[,†,§]

[†]Laboratory of Clean Energy Chemistry and Materials, Lanzhou Institute of Chemical Physics, Chinese Academy of Science, Lanzhou 730000, P. R. China

[‡]Shenyang National Laboratory for Materials Science, Institute of Metal Research, Chinese Academy of Sciences, Shenyang 110016, P. R. China

[§]State Key Laboratory of Solid Lubrication, Lanzhou Institute of Chemical Physics, Chinese Academy of Sciences, Lanzhou 730000, P. R. China

Supporting Information

**ABSTRACT:** Graphene nanoscroll (GNS) is a spirally wrapped two-dimensional (2D) graphene sheet (GS) with a 1D tubular structure resembling that of a multiwalled carbon nanotube (MWCNT). GNS provide open structure at both ends and interlayer galleries that can be easily intercalated and adjusted, which show great potential applications in energy storage. Here we demonstrate a novel and simple strategy for the large-scale preparation of GNSs wrapping $Fe_3O_4$ nanoparticles (denoted as $Fe_3O_4$@GNSs) from graphene oxide (GO) sheets by cold quenching in liquid nitrogen. When a heated aqueous mixed suspension of GO sheets and $Fe_3O_4$ nanoparticles is immersed in liquid nitrogen, the in-situ wrapping of $Fe_3O_4$ nanoparticles with GNSs is easily realized. The structural conversion is closely correlated with the initial temperature of mixed suspension, the zeta potential of $Fe_3O_4$ nanoparticles and the immersion way. Remarkably, such hybrid structure provides the right combination of electrode properties for high-performance lithium-ion batteries. Compared with other wrapping structure, such 1D wrapping structure (GNSs wrapping) effectively limits the volume expansion of $Fe_3O_4$ nanoparticles during the cycling process, consequently, a high reversible capacity, good rate capability, and excellent cyclic stability are achieved with the material as anode for lithium storage. The results presented here may pave a way for the large-scale preparation of GNS-based materials in electrochemical energy storage applications.

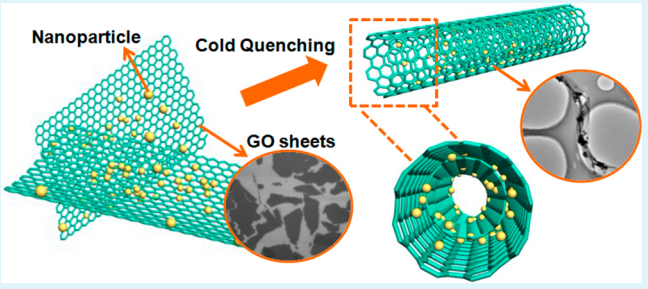


**KEYWORDS:** *graphene nanoscroll, graphene, $Fe_3O_4$, one-dimensional wrapping, lithium-ion batteries*

## INTRODUCTION

Electrode materials (i.e., anode and cathode materials) play dominant roles in the performance of lithium-ion batteries.[1] For anode materials, many materials with superior capacity, such as Si,[2,3] Sn,[4,5] and transition metal oxides ($Fe_3O_4$, $Fe_2O_3$, $Co_3O_4$, $TiO_2$, etc.),[6−14] are being studied and significant achievements have been obtained.[15] However, these high-capacity materials are still with a problem of rapid capacity fading because of pulverization during cycling, which leads to the breakdown of electrical connection of anode materials from current collectors.[15] Many strategies, such as nanostructuring, designing unique configurations, controlling pore structures, and combining micro- and nanostructures, have been employed to solve these problems.[16] Moreover, different carbons (amorphous carbon, mesoporous carbon, and carbon nanotubes) wrapping is also an efficient approach for improving electrochemical performance of the active materials in lithium-ion batteries by notable electronic conductivity improvement.[17−21] Among them, graphene is a very ideal material for improving the electrochemical performance of the active materials because of its outstanding properties, including great mechanical stiffness, strength, and elasticity, very high electrical and thermal conductivity, and large surface area.[22] For instance, most of the active materials are deposited on three-dimensional (3D) graphene foam or encapsulated as a core in graphene shell, and show excellent electrochemical performance.[22]

Received: May 3, 2014
Accepted: May 14, 2014
Published: May 14, 2014

  

Graphene nanoscroll (GNS), a new kind of graphene-based material, is a spirally wrapped 2D graphene sheet (GS) with a 1D tubular structure resembling that of a multiwalled carbon nanotube (MWCNT).[23−26] Compared with CNT, GNS provides open structure at both ends and interlayer galleries that can be easily intercalated and adjusted, which shows great potential applications in energy storage.[27−29] In addition, the open structure feature of GNS ensures the continuous conducting pathways for electrons though the electrodes and the gemometry also can promote facile strain relaxation during battery operation. Thus, the synergistic combination of GNS with structural stability, efficient electron transport pathway and metal oxide materials with superior capacity, may result in the enhancement of the electrochemical performance.[29] However, almost all of studies on the applications of GNS focus on theoretical predictions and calculations. It is mainly restricted from the difficulty in the preparation of GNS-based materials.[25,30] So far, there is only a report on the successful preparation of GNS wrapped nanomaterials.[22] In that work, $V_3O_7$ nanowires are used as the template to prepare GNS wrapped $V_3O_7$ nanowires ($V_3O_7$@GNS). The unique structure of GNS provides space for the volume expansion and shows space confining effect for inhibiting the agglomeration of $V_3O_7$ nanowire, thus leading to remarkable electrochemical properties.[22] However, this method is only suitable for preparing GNS wrapped nanowires materials.

In this paper, we demonstrate a novel and simple method for the large-scale preparation of GNSs wrapping $Fe_3O_4$ nanoparticles (denoted as $Fe_3O_4$@GNSs) from GO aqueous suspension by simple cold quenching in liquid nitrogen, freeze-drying and subsequent thermal reduction. More interestingly, the as-made $Fe_3O_4$@GNSs material provides the right combination of electrode properties for high-performance lithium-ion battery. As a consequence, a high reversible capacity, good rate capability, and excellent cyclic stability are achieved with the material as anode for lithium storage.

## EXPERIMENTAL SECTION

**Preparation of GO Sheets and $Fe_3O_4$ Nanoparticles.** First, GO sheets were respectively prepared by modified chemical exfoliation,[31] using natural flake graphite (32 mesh). $Fe_3O_4$ nanoparticles were prepared by a hydrothermal method as reported by Li et al.[32] and Ha et al.[33] Firstly, 1.35 g of $FeCl_3{\cdot}6H_2O$ was dissolved into 25 mL of ethylene glycol under stirring. Afterward, 2.7 g of sodium acetate and 1.0 g of trisodium citrate were added into the above solution with vigorous stirring. The mixed solution was transferred in a Teflon-lined autoclave (with a volume of 50 mL) and then heated at 200 °C for 10 h. After being cooled to room temperature, the precipitate was washed with ethanol and deionized water several times, and then dried at 25 °C in a vacuum oven.

**Fabrication of $Fe_3O_4$@GNSs.** The $Fe_3O_4$ aqueous dispersion (1.0 mg $mL^{-1}$, 50 mL) and the GO suspension (1.0 mg $mL^{-1}$, 120 mL) were mixed together with aid of sonication for 5 min. After that, three comparative experiments were done as follows. (1) A plastic tube with the mixed suspension was heated up to 80 °C, and then put into liquid nitrogen. The completely frozen solid was suffered the vacuum freeze-drying to remove water and then reduced by thermal treatment at 300 °C in argon atmosphere. (2) The mixed suspension was heated up to 80 °C and rapidly poured in liquid nitrogen. The following drying and reduction were the same as 1. (3) The mixed suspension was dried by traditional vacuum freeze-drying method.

In addition, to further adjust the wrapping structure of GNSs, we first surface-modified as-prepared $Fe_3O_4$ nanoparticles by dilute hydrochloric acid (HCl) and sodium citrate solutions, respectively.[34] In detail, $Fe_3O_4$ nanoparticles (1.0 g) was dispersed in 1 M HCl aqueous solution with aid of sonication for 5 min, and the upper yellow solution was removed by magnetic separation. After that, these $Fe_3O_4$ nanoparticles were dispersed in 5 wt % aqueous solution of sodium acetate under stirring for 1 h. The modified $Fe_3O_4$ nanoparticles were collected by magnetic separation followed by washing with water and dry in vacuum. Through the above process, the modified $Fe_3O_4$ nanoparticles were well-dispersed in water. Subsequently, the same process as the above 1 was run for preparing $Fe_3O_4$@GNSs. The amount of $Fe_3O_4$ nanoparticles used in this process is the same as in 1 and 2. The mass ratio between GNS and $Fe_3O_4$ is about 1:1.

**Characterization.** The morphology and structure of GNS-based samples were characterized by scanning electron microscopy (FESEM, JSM 6701F) and transmission electron microscopy (TEM, Tecnai F20, 200 kV). The structure of $Fe_3O_4$@GNSs was investigated by powder X-ray diffraction (XRD, Cu K$\alpha$ radiation, Panalytical X′ Pert Pro). In addition, the zeta potential measurements of $Fe_3O_4$ nanoparticles were carried out by Zetasizer nano3600 instrument.

**Electrochemical Measurements.** The electrochemical properties of anode materials of lithium-ion battery were evaluated by galvanostatic charge/discharge technique. Each working electrode was prepared by mixing 90 wt % active material and 10 wt % PVDF (polyvinylidene difluoride) with aid of *N*-methyl-2-pyrrolidone (NMP) to form a homogeneous slurry, which was then coated onto a copper foil and dried under vacuum at 110 °C for 10 h. The electrodes were assembled into coin cells (CR2032) in an argon-filled glove box by using 1 mol/L $LiPF_6$ in ethylenecarbonate (EC) and diethylenecarbonate (DEC) (1:1, v/v) as the electrolyte and Li metal as the counter electrode. The assembled coin cells were tested in the voltage range of 0.01-3.0 V (vs $Li/Li^+$) by using a CT2001A cell test instrument (LAND Electronic Co.). The electrochemical impedance spectroscopy (EIS) measurements were carried out over the frequency range from 100 kHz to 0.1 Hz using an electrochemical working station (CHI660D, Shanghai, China). All electrochemical measurements were carried out at 25 °C in a digital biochemical incubator and the specific capacity was calculated on the basis of the weight of anode active material (total mass of GNSs and $Fe_3O_4$ nanoparticles).

## RESULTS AND DISCUSSION

**Preparation and Characterization of $Fe_3O_4$@GNSs.** Figure 1 is the schematic diagram of the synthetic route of

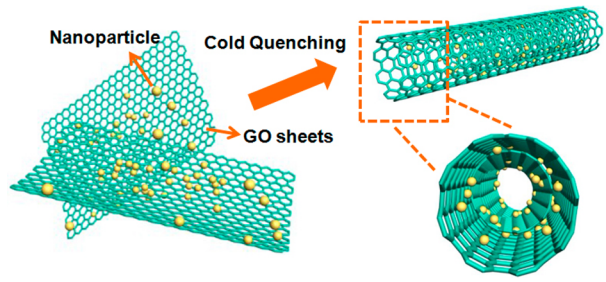


**Figure 1.** Schematic diagram of synthetic route of $Fe_3O_4$@GNSs composite.

$Fe_3O_4$@GNSs composite. GO sheets was prepared by the chemical exfoliation from graphite according to the reported method,[31] and the SEM images of the GO sheets is shown in Figure 2a. As we know, $Fe_3O_4$ anode material has attracted considerable attention because of its high theoretical specific capacity (~927 mAh $g^{-1}$), low processing cost, natural abundance as well as eco-friendliness.[15,35] In our work, we choose the $Fe_3O_4$ nanoparticles as the intercalated material. To this end, $Fe_3O_4$ nanoparticles used in our experiment were prepared by a simple hydrothermal method.[32,33,36,37] Images b


dx.doi.org/10.1021/am502574j | ACS Appl. Mater. Interfaces 2014, 6, 9890−9896

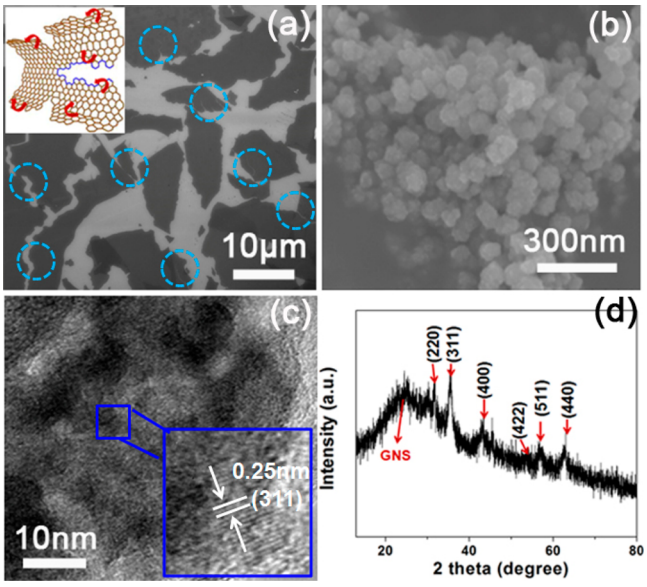


**Figure 2.** (a) SEM image of GO sheets. The circle parts in the image clearly show the cracks on GO sheets. Inset is the rolling tendency and direction of GO sheet. (b) Representative SEM image of as-made $Fe_3O_4$ nanoparticles and (c) TEM images of $Fe_3O_4$ nanoparticles. Inset is the corresponding HRTEM image. (d) XRD pattern of $Fe_3O_4$@GNSs.

and c in Figure 2 shows the SEM and TEM images of the as-made $Fe_3O_4$ nanoparticles.

The key steps for preparation $Fe_3O_4$@GNSs materials is cold quenching by liquid nitrogen (Figure 1). The mixed suspension of GO and $Fe_3O_4$ nanoparticles in a plastic box was heated up to 80 °C, the plastic box with the hot GO suspension was put into liquid nitrogen quickly for cold quenching. We consider that the nanoparticles dispersed in the GO aqueous suspension might be wrapped with GO sheets during the GO rolling process. The frozen suspension is freeze-dried, and finally the dried product was thermally reduced under an argon atmosphere. The whole experimental process is quite simple and has high output.

Following the process showed before, we can obtain the $Fe_3O_4$@GNSs materials and the results are shown in Figures 3a, 3d, 4a, and 4d (denoted as sample I). When a plastic tube with the hot GO-$Fe_3O_4$ mixed suspension is put into liquid nitrogen, the GO sheets roll up to form GNS and $Fe_3O_4$ nanoparticles intercalate into the galleries between GNS interlayers. It is worth noting that most GNSs have the diameters ranging from 400 to 800 nm. The thickness of the

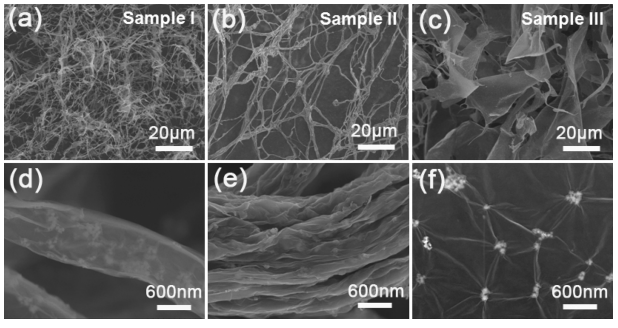


**Figure 3.** SEM images of three kinds of samples: (a, d) sample I, (b, e) sample II, and (c, f) sample III.

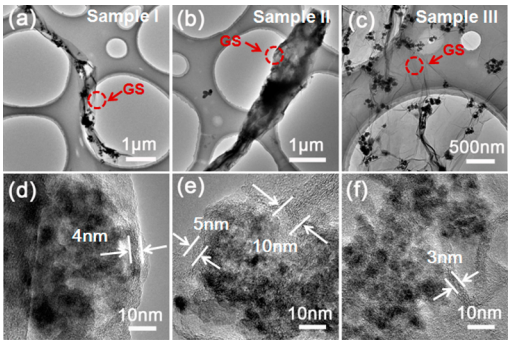


**Figure 4.** TEM images of three kinds of samples: (a, d) sample I, (b, e) sample II, and (c, f) sample III.

GNS wall is about 4 nm and the $Fe_3O_4$ nanoparticles can be viewed clearly (Figure 4a, d). Figure 2d shows its typical XRD pattern that has the signals of crystalline GNSs and $Fe_3O_4$. More interestingly, some GNSs with $Fe_3O_4$ nanoparticles connect each other to form a 3D network. As shown in Figure 2a, there are many cracks existing on the initial GO sheets due to the unavoidable breaking of GO sheets during the vigorous oxidation and exfoliation.[31] We believe that, during the cold quenching process, the GO sheets roll up along the direction of the arrow (Figure 2a inset) and the connection point is formed (see Figure S1 in the Supporting Information). These branches connected and twined with the adjacent ones to minimize the total surface energy and the 3D network of GNSs is formed.[38]

To clarify the forming process of $Fe_3O_4$@GNSs and define the key parameters during the process, we studied the relationship between the structure of product and the experimental parameters. In our study, four factors (liquid nitrogen, the temperature of the initial GO-$Fe_3O_4$ mixed suspension, the zeta potential of $Fe_3O_4$ nanoparticles and the cold quenching mode) were systematically investigated. The detailed preparation processes of different $Fe_3O_4$@GNSs samples are described in the Experimental Section. As shown in Figure S2 in the Supporting Information, when the traditional vacuum freeze-drying machine was used to freeze and dry the GO-$Fe_3O_4$ mixed suspension, the GO sheets and the $Fe_3O_4$ nanoparticles aggregate together in the product. It indicates that the extremely low temperature (about -196 °C) of liquid nitrogen is the very important key factor for the formation of $Fe_3O_4$@GNSs. As shown in Figure S3 in the Supporting Information, when a plastic tube with room-temperature GO-$Fe_3O_4$ suspension was put into liquid nitrogen, the $Fe_3O_4$ nanoparticles are not wrapped with GNSs in the corresponding product. According to the mechanism of GNS formation, the rolling process is dominated by two major energetic contributions including the increase of the elastic energy and the decrease of the free energy on a GS.[30] Therefore, on aspect of energy, when the hot GO suspension is put into the liquid nitrogen, more temperature difference is provided, resulting in that the rolling level for the hot GO suspension is much better than that for the room temperature GO suspension. The as-prepared $Fe_3O_4$ nanoparticles were firstly surface-modified by dilute hydrochloric acid and sodium citrate solutions to change the surface charges of $Fe_3O_4$ nanoparticles.[34] This modification is relative to the increase of surface negative charges of $Fe_3O_4$ nanoparticles (The zeta potential of the nanoparticles decreases from -41.2 mV to -50.1 mV). The wrapping structure of the final $Fe_3O_4$@GNSs would be obviously changed after carrying out the same process for

preparing sample I. As shown in Figures 3b, 3e, 4b, and 4e, in the final product (denoted as sample II), many GSs roll up together with $Fe_3O_4$ nanoparticles, resulting in the formation of fat fibrous structure. The thickness of the graphene wrinkle or GNS wall is 5−10 nm (Figure 4e), which is much thicker than that for the sample I. On the basis of these results, we infer that the charge amount on $Fe_3O_4$ nanoparticles plays an important role in the above rolling process. The increase charge may promote the rolling process but the concrete reason is still not clear and should be probed in the near future. As for the cold quenching mode aspect, two comparative experiments were done at the same time. When the hot GO-$Fe_3O_4$ mixed suspension was poured into liquid nitrogen directly, in the final product (denoted as sample III) as shown in Figure 3c, 3f, 4c, 4f, the $Fe_3O_4$ nanoparticles are embedded in the crinkled, thin and flexible GSs instead of GNSs. The wrinkle width is about 3 nm. This may because the mixed suspension directly poured into liquid nitrogen was frozen so quickly that the GO sheets have no time to roll up.

To verify the fact that the $Fe_3O_4$ nanoparticles exist in the interlayers instead of the center of a GNS, the sample II was put in ethanol and sonicated for 15 min in order to open the GNSs, and Figure 5 shows the TEM images of the treated sample. As

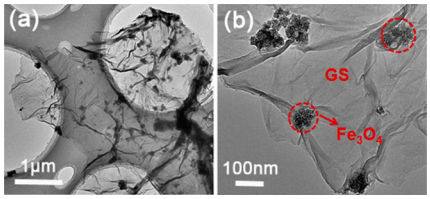


**Figure 5.** (a, b) TEM images of an opened GNS; b is the enlarged image of a.

the images show, the GNS can be opened and the $Fe_3O_4$ nanoparticles disperse on the whole sheet. It indicates that the $Fe_3O_4$ nanoparticles indeed exist in the interlayers of GNS.

**Electrochemical Performances.** As we know, the theoretical specific capacity of $Fe_3O_4$ is ~927 mAh $g^{-1}$. However, this high-capacity material is still with a problem of rapid capacity fading just as shown in Figure 6. The $Fe_3O_4$ nanoparticles used as anode material show a poor cycling life, and the discharge capacity is only 22 % of the initial capacity after 50 cycles at 0.1 C (1 *C* = 1000 mAh $g^{-1}$). Carbons (including amorphous carbon, graphene)-wrapped $Fe_3O_4$ as anode material has shown improved cyclability and rate performance compared with pure $Fe_3O_4$.[36,39−43] In our system,

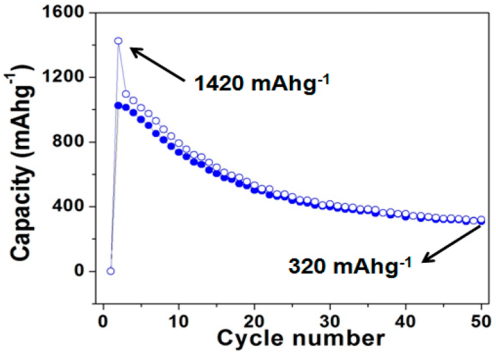


**Figure 6.** Cycling stability for the pure $Fe_3O_4$ nanoparticles at 0.1 *C*.

as shown in comparison, after the same quantity of $Fe_3O_4$ nanoparticles were wrapped with GNSs (to form sample I and sample II) or GSs (to form sample III), the electrochemical properties are remarkably improved. Figure 7 shows the electrochemical properties for the three hybrid materials. Figure 7a displays their charge/discharge profiles of the first cycle at 0.1 C. The charge and discharge curves present a voltage plateau at ~0.8 V, which closely follows earlier reports on $Fe_3O_4$ anode materials.[15,35,39] Among them, the first discharge capacity of sample I is able to reach ~1720 mAh $g^{-1}$, which is much higher than that of sample II (~1400 mAh $g^{-1}$) and sample III (~1410 mAh $g^{-1}$). Similarly, the charge capacity of sample I, sample II and sample III is about 1060, 810, and 960 mAh $g^{-1}$, respectively. The results indicate that the different wrapping type brings out entirely different electrochemical behaviors. Figure 7b shows the charge/discharge cycling performance of the three samples at a current density of 0.1 C for 50 cycles. It is clear seen that the capacity is well-retained for 1D wrapping structure of sample I (1010 mAh $g^{-1}$) and sample II (770 mAh $g^{-1}$) over 50 cycles, but the capacity of sample III (2D wrapping structure) decreases from 960 to 840 mAh $g^{-1}$ after 50 cycles. It indicates that the GNS-wrapping (1D wrapping) shows better improvement effect on the cycling stability compared with the GS-wrapping (2D wrapping). This may be due to the open ending of the GNS-wrapping structure that enables us to make the $Li^+$ transfer more easily during the charge/discharge process, and the GNSs network also enables us to provide an effective conducting network. More importantly, compared with the GSs wrapping, GNSs as a shell-type wrapping could more effectively limit the volume expansion of $Fe_3O_4$ nanoparticles during the cycling process, resulting in the excellent cycling stability. The stability of the $Fe_3O_4$ nanoparticles wrapped by GNS (sample II) is examined by TEM after 50 cycles (Figure 8). As show in images a and b in Figure 8, the particles cluster almost maintain their morphology, proving little damage caused by $Li^+$ insertion/extraction cycles. So it can be concluded that the GNS is very effective in protecting the nanoparticles. Figure 7c shows the rate capability of the three samples. As the curves show, the rate capacity of sample I is much better than that of sample II and sample III at all current rates. The specific capacity of the sample I still retains about 300 mAh $g^{-1}$ at a high rate of 5 *C*, about 33% of the initial capacity at 0.1 *C*. The outstanding rate capability also depends on its high electronic conductivity and small volume change during charge/discharge process. However, for sample II, the $Fe_3O_4$ nanoparticles cannot be utilized sufficiently since so many scrolls that act as a barrier to cut off the $Li^+$ transfer pathway, resulting in the lowest capacity at all current rates. For the sample III, the $Li^+$ can transfer from the defects or the edges on the GSs but the transfer way might be longer than that for the sample I, so that its rate performance is not as well as that of sample I. In order to prove this conclusion, the electrochemical impedance spectroscopy (EIS) was performed to experimentally probe $Li^+$ transfer resistance of these materials, and the corresponding plots are shown in Figure 7d. As the EIS profiles show, sample I exhibits the lowest charge transfer resistance, which means that it has the fastest charge transfer behavior. This result further suggests that $Fe_3O_4$@GNSs with open ending is beneficial to the $Li^+$ transfer, while the full and tight GS-wrapping is resistive to the $Li^+$ transfer, resulting in the large charge transfer resistance.[44] We also compare our results with other reported wrapping strucure of $Fe_3O_4$ ($Fe_3O_4$@graphene, $Fe_3O_4$@carbon,


dx.doi.org/10.1021/am502574j | ACS Appl. Mater. Interfaces 2014, 6, 9890−9896

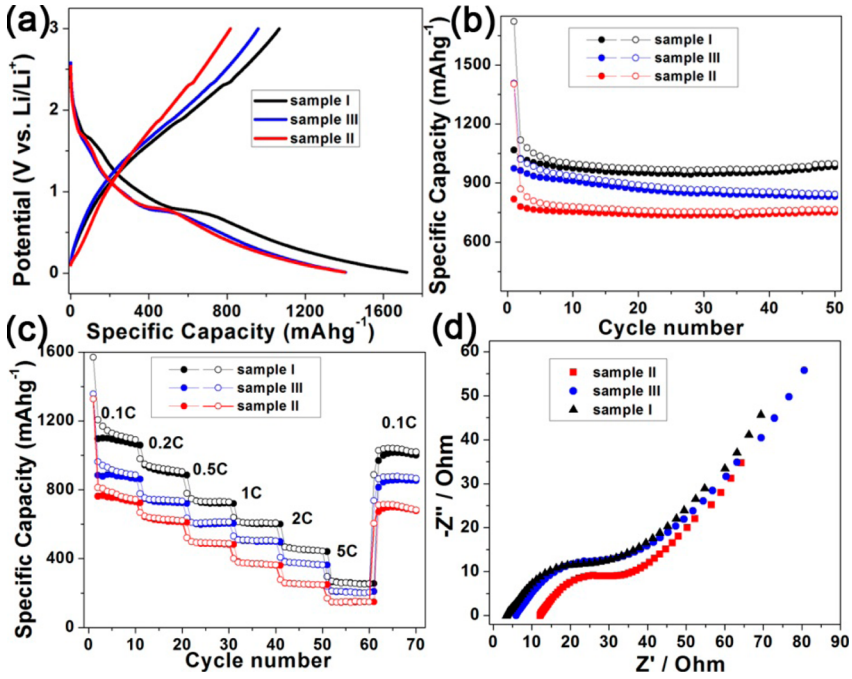


**Figure 7.** Electrochemical properties of sample I, sample II, and sample III: (a) the first charge/discharge profiles; (b) cyclic stability test at 0.1 *C*; (c) rate capability from 0.1 to 5 *C* for 10 cycles; (d) EIS presented as Nyquist plots.

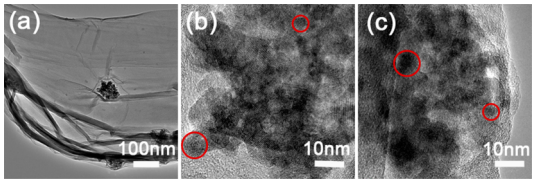


**Figure 8.** Representative TEM and HRTEM images of sample I (a, b) after 50 cycles and HRTEM images of sample I (c) before cycles. The sonication is used to disperse the electrode material (the GNS mixed with the binder which is added during the electrode prepared process), so the GNS is opened just like that shown in a. But this can not affect the $Fe_3O_4$ nanoparticle characterization.

$Fe_3O_4$@nanotube, graphene foam supported $Fe_3O_4$, and graphene@$Fe_3O_4$@carbon), and the data are shown in Table S1 in the Supporting Information. Expect for graphene foam supported $Fe_3O_4$,[45] graphene@$Fe_3O_4$@carbon[46] and $Fe_3O_4$@carbon@PGC,[47] the electrochemical performance of $Fe_3O_4$@GNSs for lithium-ion battery is better than most of previously reported works.

## CONCLUSIONS

We develop a novel and simple method for the large-scale preparation of $Fe_3O_4$@GNSs from graphene oxide (GO) sheets by cold quenching in liquid nitrogen. During the cold quenching process, GO sheets are able to roll up into GNSs and the $Fe_3O_4$ nanoparticles also intercalate in the interlayer galleries of GNS. The initial temperature of mixed suspension, the zeta potential of $Fe_3O_4$ nanoparticles and the cold quenching mode all have important effects on this structural conversion and three wrapping structures are obtained by change the parameters. The resulting three hybrid anode materials for lithium ion battery show obvious improvement on the electrochemical cycling stability compared with the pure $Fe_3O_4$ nanoparticles. Among them, the $Fe_3O_4$@GNSs (1D wrapping structure) with a few scroll cycles exhibits the best electrochemical performance including high reversible capacity, good rate capability and excellent cyclic stability. It may be due to its right structure (the open ending and the appropriate scroll cycle number) enable promote the $Li^+$ transfer and prevent the volume expansion of $Fe_3O_4$ nanoparticles. These results presented here may open up the possibility for the large-scale preparation of GNS-wrapped nanomaterials, which may be useful in high-performance energy storage devices.

## ASSOCIATED CONTENT

### Supporting Information

SEM image of GO-$Fe_3O_4$ mixed suspension dried by traditional vacuum freeze-drying and GO-$Fe_3O_4$ mixed suspension at room temperature; comparison of the electrochemical performance of $Fe_3O_4$@GNSs with other reported wrapping structures. This material is available free of charge via the Internet at http://pubs.acs.org.

## AUTHOR INFORMATION

### Corresponding Author

*E-mail: xbyan@licp.cas.cn. Tel./Fax: +931 4968055.

### Notes

The authors declare no competing financial interest.

## ACKNOWLEDGMENTS

The authors thank Miss L. L. Zhang, Mr. W. Chen, Dr W. Jiao and Dr. Z. Weng for their valuable discussions. This work was supported by the Top Hundred Talents Program of the Chinese Academy of „ Natural Science Foundation of China (21303234), China Postdoctoral Science Foundation (2013M530437) and Ministry of Science and Technology of China (2012AA030303) .

## ABBREVIATIONS

GNS, graphene nanoscroll

$Fe_3O_4$@GNSs, GNSs wrapping $Fe_3O_4$ nanoparticles

## REFERENCES


(1) Tarascon, J. M.; Armand, M. Issues And Challenges Facing Rechargeable Lithium Batteries. *Nature* **2001**, *414*, 359−367.
(2) Gao, B.; Sinha, S.; Fleming, L.; Zhou, O. Alloy Formation In Nanostructured Silicon. *Adv. Mater.* **2001**, *13*, 816−819.
(3) Chan, C. K.; Peng, H. L.; Liu, G.; McIlwrath, K.; Zhang, X. F.; Huggins, R. A.; Cui, Y. High-Performance Lithium Battery Anodes Using Silicon Nanowires. *Nat. Nanotechnol.* **2008**, *3*, 31−35.
(4) Lee, K. T.; Jung, Y. S.; Oh, S. M. Synthesis Of Tin-Encapsulated Spherical Hollow Carbon For Anode Material In Lithium Secondary Batteries. *J. Am. Chem. Soc.* **2003**, *125*, 5652−5653.
(5) Derrien, G.; Hassoun, J.; Panero, S.; Scrosati, B. Nanostructured Sn-C Composite as an Advanced Anode Material in High-Performance Lithium-Ion Batterie. *Adv. Mater.* **2007**, *19*, 2336−2340.
(6) Poizot, P.; Laruelle, S.; Grugeon, S.; Dupont, L.; Tarascon, J. M. Nano-Sized Transition-Metaloxides As Negative-Electrode Materials For Lithium-Ion Batteries. *Nature* **2000**, *407*, 496−499.
(7) Nam, K. T.; Kim, D. W.; Yoo, P. J.; Chiang, C. Y.; Meethong, N.; Hammond, P. T.; Chiang, Y. M.; Belcher, A. M. Virus-Enabled Synthesis And Assembly Of Nanowires For Lithium Ion Battery Electrodes. *Science* **2006**, *312*, 885−888.
(8) Li, Y. G.; Tan, B.; Wu, Y. Y. Mesoporous $Co_3O_4$ Nanowire Arrays for Lithium Ion Batteries with High Capacity and Rate Capability. *Nano Lett.* **2008**, *8*, 265−270.
(9) Reddy, M. V.; Yu, T.; Sow, C. H.; Shen, Z. X.; Lim, C. T.; Rao, G. V. S.; Chowdari, B. V. R. $\alpha$-$Fe_2O_3$ Nanoflakes As An Anode Material For Li-Ion Batteries. *Adv. Funct.Mater.* **2007**, *17*, 2792−2799.
(10) Chen, J.; Xu, L. N.; Li, W. Y.; Gou, X. L. Alpha-$Fe_2O_3$ Nanotubes In Gas Sensor And Lithium-Ion Battery Applications. *Adv. Mater.* **2005**, *17*, 582−586.
(11) Cui, Z. M.; Hang, L. Y.; Song, W. G.; Guo, Y. G. High-Yield Gas-Liquid Interfacial Synthesis of Highly Dispersed $Fe_3O_4$ Nanocrystals and Their Application in Lithium-Ion Batteries. *Chem. Mater.* **2009**, *21*, 1162−1166.
(12) Zhi, L. J.; Hu, Y. S.; Hamaoui, B. E.; Wang, X.; Lieberwirth, I.; Kolb, U.; Maier, J.; Mullen, K. Precursor-Controlled Formation Of Novel Carbon/Metal And Carbon/Metal Oxide Nanocomposites. *Adv. Mater.* **2008**, *20*, 1727−1731.
(13) Wang, Y.; Su, F. B.; Lee, J. Y.; Zhao, X. S. Crystalline Carbon Hollow Spheres, Crystalline Carbon-$Sno_2$ Hollow Spheres, And Crystalline $Sno_2$ Hollow Spheres: Synthesis And Performance In Reversible Li-Ion Storage. *Chem. Mater.* **2006**, *18*, 1347−1353.
(14) Lou, X. W.; Wang, Y.; Yuan, C. L.; Lee, J. Y.; Archer, L. A. Template-Free Synthesis Of $Sno_2$ Hollow Nanostructures With High Lithium Storage Capacity. *Adv. Mater.* **2006**, *18*, 2325−2329.
(15) Zhou, G. M.; Wang, D. W.; Li, F.; Zhang, L. L.; Li, N.; Wu, Z. S.; Wen, L.; Lu, M.; Cheng, H.-M. Graphene-Wrapped $Fe_3O_4$ Anode Material with Improved Reversible Capacity and Cyclic Stability for Lithium Ion Batteries. *Chem. Mater.* **2010**, *22*, 5306−5313.
(16) Liu, C.; Li, F.; Ma, L. P.; Cheng, H.-M. Advanced Materials for Energy Storage. *Adv. Mater.* **2010**, *22*, E28−E62.
(17) Fan, J.; Wang, T.; Yu, C. Z.; Tu, B.; Jiang, Z. Y.; Zhao, D. Y. Ordered, Nanostructured Tin-Based Oxides/Carbon Composite As The Negative-Electrode Material For Lithium-Ion Batteries. *Adv. Mater.* **2004**, *16*, 1432−1436.
(18) Grigoriants, I.; Sominski, L.; Li, H. L.; Ifargan, I.; Aurbach, D.; Gedanken, A. The Use Of Tin-Decorated Mesoporous Carbon As An Anode Material For Rechargeable Lithium Batteries. *Chem. Commun.* **2005**, *7*, 921−923.
(19) Kumar, T. P.; Ramesh, R.; Lin, Y. Y.; Fey, G. T. K. Tin-Filled Carbon Nanotubes As Insertion Anode Materials For Lithium-Ion Batteries. *Electrochem. Commun.* **2004**, *6*, 520−525.
(20) An, G. M.; Na, N.; Zhang, X. R.; Miao, Z. J.; Miao, S. D.; Ding, K. L.; Liu, Z. M. $SnO_2$/Carbon Nanotube Nanocomposites Synthesized In Supercritical Fluids: Highly Efficient Materials For Use As A Chemical Sensor And As The Anode Of A Lithium-Ion Battery. *Nanotechnology* **2007**, *18*, 435707.
(21) Zhang, W. M.; Wu, X. L.; Hu, J. S.; Guo, Y. G.; Wan, L. J. Carbon Coated $Fe_3O_4$ Nanospindles as a Superior Anode Material for Lithium-Ion Batteries. *Adv. Funct. Mater.* **2008**, *18*, 3941−3946.
(22) Yan, M. Y.; Wang, F. C.; Han, C. H.; Ma, X. Y.; Xu, X.; An, Q. Y.; Xu, L.; Niu, C. J.; Zhao, Y. L.; Tian, X. C. Nanowire Templated Semihollow Bicontinuous Graphene Scrolls: Designed Construction, Mechanism, and Enhanced Energy Storage Performance. *J. Am. Chem. Soc.* **2013**, *135*, 18176−18182.
(23) Viculis, L. M.; Mack, J. J.; Kaner, R. B. A Chemical Route to Carbon Nanoscrolls. *Science* **2003**, *299*, 1361.
(24) Xie, X.; Ju, L.; Feng, X. F.; Sun, Y. H.; Zhou, R. F.; Liu, K.; Fan, S. S.; Li, Q. Q.; Jiang, K. L. Controlled Fabrication of High-Quality Carbon Nanoscrolls from Monolayer Graphene. *Nano Lett.* **2009**, *9*, 2565−2570.
(25) Zheng, J.; Liu, H. T.; Wu, B.; Guo, Y. L.; Wu, T.; Yu, G.; Liu, Y. Q.; Zhu, D. B. Production of High-Quality Carbon Nanoscrolls with Microwave Spark Assistance in Liquid Nitrogen. *Adv. Mater.* **2011**, *23*, 2460−2463.
(26) Xia, D.; Xue, Q. Z.; Xie, J.; Chen, H. J.; Lv, C.; Besenbacher, F.; Dong, M. D. Fabrication of Carbon Nanoscrolls from Monolayer Graphene. *Small* **2010**, *6*, 2010−2019.
(27) Zeng, F.; Kuang, Y.; Liu, G.; Liu, R.; Huang, Z.; Fu, C.; Zhou, H. Supercapacitors based on high-quality graphene scrolls. *Nanoscale* **2012**, *4*, 3997−4001.
(28) Deng, J.; Ji, H.; Yan, C.; Zhang, J.; Si, W.; Baunack, S.; Oswald, S.; Mei, Y.; Schmidt, O. G. Naturally Rolled-up C/Si/C Trilayer Nanomembranes as Stable Anodes for Lithium Ion Batteries with Remarkable Cycling Performance. *Angew. Chem., Int. Ed.* **2013**, *52*, 2326−2330.
(29) Mai, L.; Wei, Q.; An, Q.; Tian, X.; Zhao, Y.; Xu, X.; Xu, L.; Chang, L.; Zhang, Q. Nanoscroll Buffered Hybrid Nanostructural $VO_2$ (B) Cathodes for High-Rate and Long-Life Lithium Storage. *Adv. Mater.* **2013**, *25*, 2969−2973.
(30) Braga, S. F.; Coluci, V. R.; Legoas, S. B.; Giro, R.; Galvao, D. S.; Baughman, R. H. Structure and Dynamics of Carbon Nanoscrolls. *Nano Lett.* **2004**, *4*, 881−884.
(31) Zhao, J. P.; Pei, S. F.; Ren, W. C.; Gao, L. B.; Cheng, H. M. Efficient Preparation of Large-Area Graphene Oxide Sheets for Transparent Conductive Films. *ACS Nano* **2010**, *4*, 5245−5252.
(32) Deng, H.; Li, X. L.; Peng, Q.; Wang, X.; Chen, J. P.; Li, Y. D. Monodisperse Magnetic Single-Crystal Ferrite Microspheres. *Angew. Chem., Int. Ed.* **2005**, *44*, 2782−2785.
(33) Dong, F. P.; Guo, W. P.; Bae, J. H.; Kim, S. H.; Ha, C. S. Highly Porous, Water-Soluble, Superparamagnetic, and Biocompatible Magnetite Nanocrystal Clusters for Targeted Drug Delivery. *Chem.—Eur. J.* **2011**, *17*, 12802−12808.
(34) Hong, R. Y.; Li, J. H.; Zhang, S. Z.; Li, H. Z.; Zheng, Y.; Ding, J. M.; Wei, D. G. Preparation and Characterization of Silica-Coated $Fe_3O_4$ Nanoparticles Used as Precursor of Ferrofluids. *Appl. Surf. Sci.* **2009**, *255*, 3485−3492.
(35) Taberna, L.; Mitra, S.; Poizot, P.; Simon, P.; Tarascon, J. M. High Rate Capabilities $Fe_3O_4$-Based Cu Nano-Architectured Electrodes for Lithium-Ion Battery Applications. *Nat. Mater.* **2006**, *5*, 567−573.
(36) Chen, H. M.; Deng, C. H.; Zhang, X. M. Synthesis of $Fe_3O_4$@$SiO_2$@PMMA Core-Shell-Shell Magnetic Microspheres for Highly Efficient Enrichment of Peptides and Proteins for MALDI-ToF MS Analysis. *Angew. Chem., Int. Ed.* **2010**, *49*, 607−611.
(37) Liu, J.; Sun, Z. K.; Deng, Y. H.; Zou, Y.; Li, C. Y.; Guo, X. H.; Xiong, L. Q.; Gao, Y.; Li, F. Y.; Zhao, D. Y. HighlyWater-Dispersible Biocompatible Magnetite Particles with Low Cytotoxicity Stabilized by Citrate Groups. *Angew. Chem., Int. Ed.* **2009**, *48*, 5875−5879.
(38) Mirsaidov, U.; Mokkapati, V. R. S. S.; Bhattacharya, D.; Andersen, H.; Bosman, M.; Zyilmazcdg, B. Ö; Matsudaira, P. Scrolling Graphene into Nanofluidic Channels. *Lab Chip* **2013**, *13*, 2874−2878.
(39) Zhang, W. M.; Wu, X. L.; Hu, J. S.; Guo, Y. G.; Wan, L. J. Carbon Coated $Fe_3O_4$ Nanospindles as a Superior Anode Material for Lithium-Ion Batteries. *Adv. Funct. Mater.* **2008**, *18*, 3941−3946.

(40) Yuan, S. M.; Zhou, Z.; Li, G. Structural Evolution From Mesoporous Alpha-$Fe_2O_3$ To Fe3O4@C And Gamma-Fe2O3 Nanospheres And Their Lithium Storage Performances. *CrystEngComm* **2011**, *13*, 4709−4713.
(41) Muraliganth, T.; Murugan, A. V.; Manthiram, A. Facile Synthesis Of Carbon-Decorated Single-Crystalline $Fe_3O_4$ Nanowires And Their Application As High Performance Anode In Lithium Ion Batteries. *Chem. Commun.* **2009**, *47*, 7360−7362.
(42) Wang, R. H.; Xu, C. H.; Sun, J.; Gao, L.; Lin, C. C. Flexible Free-Standing Hollow $Fe_3O_4$/Graphene Hybrid Films For Lithium-Ion Batteries. *J. Mater. Chem. A* **2013**, *1*, 1794−1800.
(43) Dong, Y. C.; Maa, R. G.; Hua, M. J.; Cheng, H.; Tsang, C. K.; Yang, Q. D.; Li, Y. Y.; Zapien, J. A. Scalable Synthesis Of $Fe_3O_4$ Nanoparticles Anchored On Graphene As A High-Performance Anode For Lithium Ion Batteries. *J. Solid State Chem.* **2013**, *201*, 330−337.
(44) Wei, W.; Lv, W.; Wu, M. B.; Su, F. Y.; He, Y. B.; Li, B. H.; Kang, F. Y.; Yang, Q. H. The Effect of Graphene Wrapping on the Performance of $LiFePO_4$ for a Lithium Ion Battery. *Carbon* **2013**, *57*, 530−536.
(45) Luo, J.; Liu, J.; Zeng, Z.; Ng, C.; Ma, L.; Zhang, H.; Lin, J.; Shen, Z.; Fan, H. Three-Dimensional Graphene Foam Supported $Fe_3O_4$ Lithium Battery Anodes with Long Cycle Life and High Rate Capability. *Nano Lett.* **2013**, *13*, 6136−6143.
(46) Su, Y.; Li, S.; Wu, D.; Zhang, F.; Liang, H.; Gao, P.; Cheng, C.; Feng, X. Two-Dimensional Carbon-Coated Graphene/Metal Oxide Hybrids for Enhanced Lithium Storage. *ACS Nano* **2012**, *9*, 8349−8356.
(47) He, C.; Wu, S.; Zhao, N.; Shi, C.; Liu, E.; Li, J. Carbon-Encapsulated $Fe_3O_4$ Nanoparticles as a High-Rate Lithium Ion Battery Anode Material. *ACS Nano* **2013**, *5*, 4459−4469.